ChemComm

Cite this: *Chem. Commun.*, 2012, **48**, 2873–2875

www.rsc.org/chemcomm

COMMUNICATION

Dual polarisation interferometry for real-time, label-free detection of interaction of mercury(II) with mercury-specific oligonucleotides†

Yong Wang,[ab] Yu Zheng,[ab] Fan Yang[a] and Xiurong Yang*[a]

Received 10th October 2011, Accepted 19th January 2012
DOI: 10.1039/c2cc16279b

A real-time, label-free dual polarisation interferometry technique was used to investigate the interaction of Hg^{2+} with a 21-mer T-rich oligonucleotide and further construct a Hg^{2+} biosensor based on thymine–Hg^{2+}–thymine coordination chemistry.

Mercury is considered one of the highly toxic heavy metal ions because of its severe adverse or irreversible impacts on human health and the environment.[1] To date, a possible molecular mechanism underlying mercury toxicity has been suggested to be the direct interaction of mercury ions with DNA molecules.[2] Therefore, during the past few decades, investigations directed to an understanding of the structural, kinetic and thermodynamic details of the interaction between mercury ions and DNA have become an increasingly active field of research.[3] Very recently, much work has revealed that synthetic thymine-rich oligonucleotides interacted specifically with Hg^{2+} based on Hg^{2+}-mediated thymine–thymine mismatch (T–Hg^{2+}–T) base pairs, accompanying the structural variation of oligonucleotides from random coil single-stranded to duplex or hairpin-like conformation.[4] Following the T–Hg^{2+}–T chemistry, considerable efforts have been dedicated to fabricating various robust biosensors for sensitive and selective detection of Hg^{2+}.[5] However, all transduction platforms only give a simple sensor response function, but cannot simultaneously provide both kinetics and structural information on the interaction of Hg^{2+} with thymine-rich oligonucleotides.

One powerful technique that not only embodies a sensor response function but also simultaneously monitors both the kinetics and structural information is dual polarisation interferometry (DPI). Dual polarisation interferometry, which has been commercialized in 2000 by Farfield Group Ltd., is a real-time, label-free, evanescent wave-based technique which allows unambiguously quantitative monitoring of changes in mass, refractive index (RI) and thickness on a sensor surface due to the binding of the analyte to the immobilized ligand.[6] An explanation on the instrument and technique can be found in ESI.† Previously, it was reported that the technique could reliably detect molecules below 50 Da.[7] To date, the DPI technique has been applied to investigate various biomolecular systems.[8] These measurements successfully reveal structural information about the biomolecular interactions taking place as the packing (from the RI) and molecule dimension (from the thickness) change, and typically give a link between a molecule's structure and its function.

In this communication, we utilized the technique to study the interaction of Hg^{2+} with a T-rich oligonucleotide and further construct the Hg^{2+} biosensor. A previously reported 21-mer oligonucleotide sequence (5′-TTC TTT CTT CCC TTG TTT GTT-3′) containing two T-rich segments spaced by three consecutive cytosine bases in the middle[5a–c] was selected as a mercury-specific oligonucleotide (MSO) probe. For comparison purposes, its complementary oligonucleotide (5′-AAC AAA CAA GGG AAG AAA GAA-3′, labelled with cMSO) was chosen as a control probe. Scheme 1 displays the fabrication of biosensing interface and detection of Hg^{2+}. A highly charged polycation, poly(ethylenimine) (PEI), is assembled onto a negatively charged bare silicon oxynitride chip surface *via* electrostatic interaction. Then, MSO with negative charges is electrostatically adsorbed onto the PEI layer. The addition of Hg^{2+} to the MSO immobilized surface greatly interferes with the surface layer structure due to the Hg^{2+}-induced conformational change of MSO from random coil single-stranded to hairpin-like structure based on T–Hg^{2+}–T chemistry. As a result, the changes in layer thickness, mass and refractive index (RI) given by DPI during the whole process can be directly

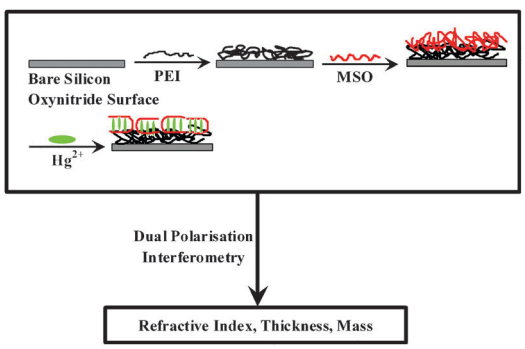

Scheme 1 Construction of biosensing interface and detection of Hg^{2+} by the dual polarisation interferometry technique.

[a] *State Key Laboratory of Electroanalytical Chemistry, Changchun Institute of Applied Chemistry, Chinese Academy of Sciences, Changchun, Jilin 130022, China. E-mail: xryang@ciac.jl.cn; Fax: +86 431 85689278; Tel: +86 431 85262056*
[b] *Graduate School of the Chinese Academy of Sciences, Beijing 100039, China*

† Electronic supplementary information (ESI) available: Explanation on DPI instrument and technique, experimental details, Fig. S1–S6 and Table S1. See DOI: 10.1039/c2cc16279b

employed to understand the Hg^{2+}/MSO interaction, reveal the corresponding structural information and further develop the Hg^{2+} biosensor.

To confirm the rationality of the mercury-specific oligonucleotide probe and the control probe, circular dichroism (CD) spectra experiments were carried out to monitor the conformational change of oligonucleotide with and without Hg^{2+}. The CD spectra of MSO and cMSO in the absence and presence of Hg^{2+} are displayed in Fig. S1A and B (ESI†) respectively. As can be seen in Fig. S1A (ESI†), MSO presents a CD spectrum with a positive band around 285 nm and an adjacent negative band around 255 nm. Addition of Hg^{2+} to MSO resulted in a red-shift together with a reduction in intensity of the positive peak. All these phenomena are similar to those discussed in earlier studies,[5c,d] strongly supporting the notion that MSO changes its conformation from random coil single-stranded to compact hairpin-like in the presence of Hg^{2+}. Almost no change in the CD spectra of cMSO before and after the addition of Hg^{2+} was observed in Fig. S1B (ESI†), indicating no conformational change of cMSO in the presence of Hg^{2+}.

Fig. 1 shows the real-time measurements of the thickness, mass and RI for the entire immobilization process with DPI. Derived from Fig. 1, the changes in layer thickness or RI are plotted against the mass loading of PEI or MSO or cMSO in order to clearly measure the extent of changes in each layer (Fig. S2, ESI†). As can be noted from Fig. 1 and Fig. S2 (ESI†), upon the injection of PEI, the initial adsorption rate was very fast, during which a sharp increase in thickness and mass loading was accompanied by a rapid decrease in RI, confirming the binding of PEI to the bare silicon oxynitride surface. After the initial period, the adsorption started to decrease slowly until attaining equilibrium, indicating an "overshoot" effect.[9a] Similarly, MSO seems to undergo such a process. However, cMSO exhibits a little difference in the whole adsorption process. After the fast initial adsorption, it took very long time for cMSO to adsorb to the maximum level, suggesting that cMSO possibly underwent slow structural and orientational rearrangements.

The key parameters (RI, thickness and mass) for the stable MSO/PEI and cMSO/PEI layers are listed in Table S1 (ESI†). It can be clearly seen that oligonucleotide layers (MSO and cMSO) have lower RI than PEI layers, implying that oligonucleotide

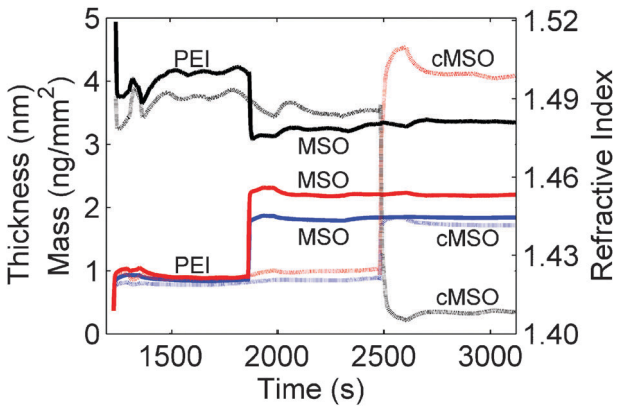

Fig. 1 Real-time DPI measurements of thickness (red line), mass (blue line) and refractive index (black line) during the immobilization of PEI and MSO (solid line) or cMSO (dashed line) on the bare silicon oxynitride surface.

layers are more water-swollen. The mass loadings of MSO and cMSO are approximately equal to that of PEI. The mass ratio of MSO or cMSO to PEI is close to the 1 : 1 mass ratio between DNA and PEI reported previously,[9] approximately following the 1 : 1 charge equivalence. Furthermore, a cMSO layer has higher thickness and lower RI than an MSO layer. The differences in layer thickness and RI are very likely to be due to different interactions of MSO or cMSO with a PEI layer. MSO and cMSO possess two thirds of thymine base and adenine base in their sequence, respectively. The adenine base has larger hydrophobicity and larger persistence length than the thymine base,[10] and as a result, in comparison with MSO, cMSO interacts with PEI layer more weakly, resulting in a thicker and looser layer. Previous literature reported that an oligonucleotide strand was about 1.9 nm wide, and each base contributed approximately 0.33 nm in length.[11] The length of a 21-mer oligonucleotide molecule could be herein calculated to be about 6.93 nm. As can be noted from Table S1 (ESI†), the addition of MSO or cMSO contributed to an increase of layer thickness by 1.32 nm and 3.44 nm, respectively. For MSO, the increase in layer thickness is below the width or the length of MSO, indicating that MSO molecules possibly adsorb "flat" onto the PEI layer and insert themselves partly into the PEI layer. For cMSO, the increase in layer thickness is below the length of cMSO and above the width of cMSO, suggesting that cMSO molecules may not be adsorbed onto the PEI layer in any extreme conformation (a "flat on" conformation or an "end on" conformation) but rather in intermediate conformations. In addition, for a 21-mer oligonucleotide molecule, the theoretical saturated surface area per molecule adsorbed on the surface in a "flat-on" conformation or an "end-on" conformation corresponds to 13.2 nm^2 and 3.6 nm^2, respectively. Based on the actual mass loading provided by DPI, we can possibly estimate the actual surface area per molecule adsorbed on the surface. Table S1 (ESI†) lists that the mass loadings are 1.007 ng mm^{-2} for MSO and 0.958 ng mm^{-2} for cMSO, respectively, which are equivalent to an area per MSO molecule of 10.4 nm^2 and an area per cMSO molecule of 11.4 nm^2. These actual areas per molecule for MSO and cMSO are slightly less than those theoretical areas adsorbed on the surface in a "flat-on" conformation, suggesting that most oligonucleotide molecules are likely to be adsorbed as a predominantly flat monolayer onto the PEI surface.

To further characterize the layer growth, another technique, atomic force microscopy (AFM), is used to directly determine the layer thickness. Typical AFM images of PEI, MSO/PEI and cMSO/PEI layers on the bare silicon surface are displayed in Fig. S3 (ESI†). On the basis of more than 50 measurements in each AFM image, the thickness for PEI, MSO/PEI and cMSO/PEI layers could be estimated to be 1.5 ± 0.6 nm, 2.9 ± 1.2 nm and 4.8 ± 2.5 nm, respectively. The thickness for all layers is similar to those values obtained using the DPI technique. The difference in thickness between the two techniques may be due to different sample preparation procedures and different surface compositions.

To study the Hg^{2+}/MSO interaction, we injected Hg^{2+} with different concentrations ranging from 0.1 to 3 μM into the immobilized MSO/PEI layer. The corresponding real-time mass, thickness and RI changes are showed in Fig. S4 (ESI†). After the addition of Hg^{2+}, the layer mass and thickness

increased while layer RI changed a little. It is worth noting that the increase in layer thickness after the addition of Hg^{2+} may be due to the structural variation of MSO from random coil to rigid hairpin-like conformation, which agrees well with those earlier observations that double-stranded DNA formed a thicker layer on top of the polymer layer than single-stranded DNA.[8a] The association rate constant, the dissociation rate constant and the association constant between Hg^{2+} and MSO could be calculated using the mass binding curves. The association (k_a) and dissociation (k_d) rate constants were estimated to be 1.92×10^4 M^{-1} s^{-1} and 0.014 s^{-1}, respectively. Derived from the kinetic constants (k_a and k_d), the association constant (K_a) was calculated to be 1.4×10^6 M^{-1}, which is in approximate accordance with other studies.[4,5e] Simultaneously, by analyzing the increase in mass at 210 s with the Hg^{2+} concentration, we obtained a linear relationship between mass increase and Hg^{2+} concentration over a range of 0.1–3.0 μM. The mass increase could be fitted as the equation M (ng mm^{-2}) = 0.013 c (μM) + 0.009 (correlation coefficient r = 0.998). The detection limit was 27 nM (S/N = 3), which agreed well with the toxicity level of Hg^{2+} in drinking water (30 nM) regulated by World Health Organization (WHO).

To further demonstrate the specific binding between Hg^{2+} and MSO, we performed the control experiments using cMSO instead of MSO. As can be noted from Fig. S5 (ESI†), compared with the MSO/PEI layer, the cMSO/PEI layer underwent a little mass change upon the addition of Hg^{2+}, indicating that MSO is a specific probe for Hg^{2+}. Then, we investigated the selectivity of the biosensor for Hg^{2+} over other individual metal ions and the mixture of all metal ions with and without Hg^{2+} (Fig. S6, ESI†). It can be clearly seen in Fig. S6 (ESI†) that each individual metal ion (Mg^{2+}, Ca^{2+}, Mn^{2+}, Fe^{3+}, Cd^{2+}, Co^{2+}, Ni^{2+}, Zn^{2+} or Pb^{2+}) and their mixture have only slight or negligible effect on the layer mass change compared with that of Hg^{2+} alone and the mixture of these metal ions with Hg^{2+}, suggesting that the biosensor has high selectivity toward Hg^{2+}. We suppose that the good selectivity of the Hg^{2+} biosensor may be mainly because Hg^{2+} can stabilize the T–T mismatches in the MSO oligonucleotide to form T–Hg^{2+}–T complexes. In addition, the mixture of these metal ions with Hg^{2+} exhibits the reduction of mass change in the surface layer compared with Hg^{2+} alone. This comparison essentially indicates that the detection limit for the Hg^{2+} biosensor in the presence of various other metal ions may be greater than that without other metal ions.

In summary, we reported the first demonstration for applying the real-time and label-free DPI technique to detect the interaction of Hg^{2+} with a T-rich oligonucleotide (MSO) as a recognition element. Not only can the DPI technique give a simple sensor response function but, more importantly, provide both kinetics and structural information. In addition, the unmodified DPI chip can be used repeatedly by using oxidizing piranha cleaning solution. Through the technique, the kinetic and thermodynamic constants of the Hg^{2+}/MSO interaction could be easily obtained. The biosensor for Hg^{2+} possessed a lower detection limit due to the high sensitivity of the DPI technique and provided high selectivity due to the specific binding ability of thymine bases to Hg^{2+}. It is expected that the biosensing strategy can be expanded to detect a variety of target molecules by using other different functional DNAs (aptamers or DNAzymes), simultaneously investigate the interaction between them and reveal the structural characteristics of functional DNA with and without targets. Future work will be done to optimize the experimental conditions or develop more robust immobilization techniques in order to create a well-defined biosensor surface.

This work was supported by the National Natural Science Foundation of China (21175124, 20890022) and the National Key Basic Research Development Project of China (2010CB933602).

Notes and references

1 (*a*) M. Hutton, in *Lead, Mercury, Cadmium and Arsenic in the Environment*, ed. T. C. Hutchinson and K. M. Meema, John Wiley & Sons, New York, 1987; (*b*) E. M. Nolan and S. J. Lippard, *Chem. Rev.*, 2008, **108**, 3443.

2 (*a*) I. Onyido, A. R. Norris and E. Buncel, *Chem. Rev.*, 2004, **104**, 5911; (*b*) C. Baird and M. Cann, W. H. Freeman, New York, 4th edn, 2008.

3 (*a*) S. Aktipis and W. W. Martz, *Fed. Proc.*, 1969, **28**, 833; (*b*) N. A. Froystein and E. Sletten, *J. Am. Chem. Soc.*, 1994, **116**, 3240; (*c*) Y. Li, Y. Jiang and X. P. Yan, *Anal. Chem.*, 2006, **78**, 6115.

4 (*a*) H. Torigoe, A. Ono and T. Kozasa, *Chem.–Eur. J.*, 2010, **16**, 13218; (*b*) C. K. Chiang, Y. W. Lin, C. C. Hu and H. T. Chang, *J. Am. Soc. Mass Spectrom.*, 2009, **20**, 1834; (*c*) H. Torigoe, Y. Miyakawa, A. Ono and T. Kozasa, *Thermochim. Acta*, 2011, DOI: 10.1016/j.tca.2011.03.018.

5 (*a*) Y. Wang, F. Yang and X. R. Yang, *ACS Appl. Mater. Interfaces*, 2010, **2**, 339; (*b*) D. Li, A. Wieckowska and I. Willner, *Angew. Chem., Int. Ed.*, 2008, **47**, 3927; (*c*) J. P. Xu, Z. G. Song, Y. A. Fang, J. Mei, L. Jia, A. J. Qin, J. Z. Sun, J. A. Ji and B. Z. Tang, *Analyst*, 2010, **135**, 3002; (*d*) Y. G. Wu, S. S. Zhan, L. R. Xu, W. W. Shi, T. Xi, X. J. Zhan and P. Zhou, *Chem. Commun.*, 2011, **47**, 6027; (*e*) Z. D. Wang, J. H. Lee and Y. Lu, *Chem. Commun.*, 2008, 6005; (*f*) W. W. Ma, C. L. Hao, W. Ma, C. R. Xing, W. J. Yan, H. Kuang, L. B. Wang and C. L. Xu, *Chem. Commun.*, 2011, **47**, 12503; (*g*) Z. Z. Lin, X. H. Li and H. B. Kraatz, *Anal. Chem.*, 2011, **83**, 6896; (*h*) L. B. Zhang, T. Li, B. L. Li, J. Li and E. K. Wang, *Chem. Commun.*, 2010, **46**, 1476; (*i*) C. W. Liu, C. C. Huang and H. T. Chang, *Anal. Chem.*, 2009, **81**, 2383.

6 (*a*) G. H. Cross, N. J. Freeman and M. J. Swann, in *Handbook of Biosensors and Biochips*, ed. R. S. Marks, C. R. Lowe, D. C. Cullen, H. H. Weetall and I. Karube, John Wiley & Sons, New York, 2007, vol. 1, ch. 32, pp. 1–20; (*b*) G. H. Cross, Y. T. Ren and N. J. Freeman, *J. Appl. Phys.*, 1999, **86**, 6483.

7 K. Karim, J. D. Taylor, D. C. Cullen, M. J. Swann and N. J. Freeman, *Anal. Chem.*, 2007, **79**, 3023.

8 (*a*) J. Wang, X. W. Xu, Z. X. Zhang, F. Yang and X. R. Yang, *Anal. Chem.*, 2009, **81**, 4914; (*b*) M. Swann, N. Freeman, S. Carrington, G. Ronan and P. Barrett, *Lett. Pept. Sci.*, 2003, **10**, 487.

9 (*a*) X. B. Zhao, Z. Q. Zhang, F. Pan, Y. H. Ma, M. P. Armes, A. L. Lewis and J. R. Lu, *Langmuir*, 2005, **21**, 9597; (*b*) X. B. Zhao, F. Pan and J. R. Lu, *Prog. Nat. Sci.*, 2005, **15**, 56.

10 (*a*) S. Akca, A. Foroughi, D. Frochtzwajg and H. W. C. Postma, *PloS One*, 2011, **6**, e18442; (*b*) J. B. Mills, E. Vacano and P. J. Hagerman, *J. Mol. Biol.*, 1999, **285**, 245.

11 A. P. R. Johnston, E. S. Read and F. Caruso, *Nano Lett.*, 2005, **5**, 953.